Scientific Inquiry and Review (SIR)
Volume 9 Issue 4, 2025
ISSN$_{(P)}$: 2521-2427, ISSN$_{(E)}$: 2521-2435
Homepage: https://journals.umt.edu.pk/index.php/SIR

Significance of Exponential Space-Based Internal Heat Source on Bio-Convective Maxwell Nanofluid Flow Due to Stretching Sheet in the Presence of Darcy–Forchheimer and Lorentz Forces

Author (s): Muhammad Arbaz[1], Muhammad Khurshid Azam[2], Muhammad Imran[1]

Affiliation (s): [1]Government College University, Faisalabad, Pakistan.
[2]Government Graduate College Satiana Road, Faisalabad, Pakistan.

Academic Editor Abaid ur Rehman

DOI: https://doi.org/10.32350/sir.94.02

History: Received: September 03, 2025, Revised: October 06, 2025, Accepted: October 27, 2025, Published: December 15, 2025

Citation: Arbaz M, Azam MK, Imran M. Significance of Exponential Space-Based Internal Heat Source on Bio-Convective Maxwell Nanofluid Flow Due to Stretching Sheet in the Presence of Darcy–Forchheimer and Lorentz Forces. *Sci Inq Rev*. 2025;9(4): 07–32. https://doi.org/10.32350/sir.94.02

Conflict of Interest: Author(s) declared no conflict of interest

A publication of
The School of Science
University of Management and Technology, Lahore, Pakistan

Significance of Exponential Space-Based Internal Heat Source on Bio-Convective Maxwell Nanofluid Flow Due to Stretching Sheet in the Presence of Darcy–Forchheimer and Lorentz Forces

Muhammad Arbaz[1*], Muhammad Khurshid Azam[2], and Muhammad Imran[1]

[1]Department of Mathematics, Government College University Faisalabad, Pakistan
[2]Department of Mathematics, Government Graduate College Satiana Road, Faisalabad, Pakistan

ABSTRACT

This study investigates two-dimensional flow of bio-convective Maxwell nanofluid over a stretching sheet in the influence of motile microorganisms. Furthermore, the impact of thermal radiation and exponential space-based heat sources have been analyzed. The results showed that magnetic, Darcy–Forchheimer, Deborah and inertia parameters significantly suppressed the velocity field while modifying thermal and concentration boundary-layer thicknesses. Brownian motion and thermophoretic effects enhanced temperature and nanoparticle concentration, whereas bioconvective parameters strongly regulated microorganism density and associated bio-convective patterns. Applications of the current research study include model oil reservoirs, solar energy technology, re-entry of spacecraft, electrical power generation, cosmological flows, chemical engineering, air and water management systems, industrial zones, human blood flow, bioindustrial systems, environmental sciences and power generating systems, *etc*.

Keywords: bioconvection, Darcy–Forchheimer, exponential space-based, Lorentz Forces, Maxwell nanofluid

Highlights

- This study shed-light on how a Maxwell nanofluid with motile microorganisms flows and transfers heat over a stretching sheet under magnetic and Darcy–Forchheimer effects
- Key parameters like magnetic field, radiation, Brownian motion, thermophoresis, and bio-convection numbers are shown to control velocity, temperature, nanoparticle concentration, and microorganism distribution in the fluid

*Corresponding Author: marbazg247@gmail.com

- The results provide guidance for designing thermal and flow systems in applications specifically but not limited to oil reservoirs, energy devices, environmental and bio-industrial processes

1. INTRODUCTION

A substance is said to be fluid if it continuously flows or deforms, when subjected to tangential stress or an outsider force. In a wide range of scientific, technical, and medicinal applications, fluid flows are crucial research topics. Numerous effects of fluid flow caused by stretched surfaces moving are felt throughout the physical universe. Such a study considers the thermal stability of chemical reactors as well as the project of thermal sub systems for use in condensers, centrifuges, separation systems, reservoirs, heat converters, cooling generating devices, and heat tubes. Nanofluids are made by mixing nanomaterials in common transporter liquids like ethylene glycol, argon, or oil. Since nanofluids are becoming more and more valuable in a variety of sectors, including sophisticated nuclear systems and nano-drug delivery, many researchers have employed them widely. These fluids also cool various heat transmission appliances, such as heat transformers and electronic freezing systems. Many researchers are attracted to convective nanofluid heat transfer flow because it has applications in almost every area of engineering and research. These include enhancing the electrical properties of lubricants with diamond and silica nanomaterials, using liquids with nanoparticles to involve light in solar panels, and using zinc and titanium oxide particles' antibacterial capabilities in biomedical production uses.

Akinshilo et al. [1] investigated the thermal examination for sodium alginate radiative nanoliquid flow. The earliest uses of nanofluids include medication administration, microelectronic fuel cells, oil recovery, lubrication, electronic cooling systems, and magnetic cell splitting, according to Jakati et al. [2]. Yusuf et al.'s [3] investigation of the effects of MHD and bioconvection, along with entropy optimization, took into consideration Williamson nanofluid employing the tilted surface inhabited by gyrotactic microorganisms. The nanofluid across a sheet that is not linearly expanding was explained by Hady et al. [4]. Slip flow and radiative heat transition over nanofluids were investigated by Souayeh et al. [5]. The effects of radiative heat flux on Maxwell nanoliquid flow over a spiraling disk that has had a chemical reaction were examined by Ahmed et al. [6]. The MHD Maxwell fluid flow with nanoparticles by rapidly increasing

surface is calculated by Farooq et al. [7]. In permeable media, squeezed flow and the heat transmission features of nanofluid flow were explored by Mahmood et al. [8]. To improve bioconvection in the creation of continuous models, Pedley et al. [9] suspended gyrotactic microorganisms. Rashad et al. [10] recently characterized the steady mixed convection boundary layer movement as taking place in a stream that is traveling vertically upward and embedded in porous material that is occupied with a nanoliquid in order to deal with thermal convective boundary condition. The flow and radiative heat transmission of a nanoliquid across a stretched sheet with temperature spike and velocity slip in porous media were covered by Zheng et al. [11]. Aziz et al. [12] calculated the result for a 3-D viscous nanoliquid flow via a spinning disk. Professionals in several disciplines of research are interested in the issue since rotational form flow has numerous applications in many different fields.

Heat transfer rates influenced by radiation are essential for the manufacturing of nuclear power plants, gas turbines, airplanes, satellites, missiles, spacecraft, and other large-scale industrial components. Many researchers are involved in learning more about the possessions of the magnetic field because of the various applications it has in the blood flow, electrical furnace, nuclear reactors, turbo equipment, installation of nuclear accelerators, and many other areas. In addition, solar energy technology, space vehicle re-entry, electrical power production, cosmological flows, and other engineering areas benefit from the heat transformation investigation of boundary layer flows with radiation. It is now possible to access the substantial literature on flows in the existence of radiation impacts. Chu et al. [13] studied radiative heat flow and Cattaneo-Christov heat flow on Maxwell nanofluid across a cylinder. The effects of Newtonian warming system and slide on Maxwell fluid with natural convection were investigated by Zhang et al. [14]. They used the Laplace transform to help them calculate analytical solutions. When heat radiation and viscous dissipation were present, Lund et al. [15] examined the dynamics of a hybrid nanoliquid flow over a stretched surface and discovered two categories of solutions. Wakif et al. [16] carried out the numerical solution of an unsteady Couette nanofluid flow under the impact of heat radiation. The irregular magnetohydrodynamic natural convection transformation of mass and temperature across a porous media sheet under the influence of thermal radiation and thermo-diffusion significances was investigated by Sharma et al. [17] using the Laplace transform approach.

Shafiq et al. [18] explored the flow of a third-grade nanofluid across an overextended cylinder. Abbas et al. [19] deliberated the influence of the slip conditions on the micro polar hybrid nanofluid flowing through the Riga channel. Nanofluid applications in a cubical enclosure with magnetic force were covered by Kolsi et al. [20] in their examination. By following heat transfer, Darcy-Forchheimer flow, and viscous dissipation, Sheikhsolami et al. [21] investigated the outcomes of magnetic field-assisted nanofluid and thermal transmission. Reiner-Philip fluid was investigated by Kumar et al. [22]. These subjects were the focus of Tlili et al.'s [23] study on Williamson nanoliquid and physical features of double chemical reactions with MHD linked with Darcy-Forchheimer, and entropy generation on a non-linearly stretched medium. The Darcy-Forchheimer flow via a changing thicker disc with entropy production was observed by Khan et al. [24] using a second order velocity slip. Khan et al. [25] studied the effects of entropy analysis, viscosity dissipation, and Joule heating while addressing the Darcy-Forchheimer flow of CNTs across a curved stretched sheet.

The term "bioconvection" refers to the macroscopic convective movement of a fluid driven by the coordinated collective swimming of microorganisms and controlled by the density difference. Now a days, microorganisms found in nanofluid are a fascinating study tool. The process of bioconvection, which is used in the production of pharmaceuticals, sedimentary waterways, microfluidic devices, lubrication things, hydrodynamics systems, polymer manufacturing, hydrodynamics fabrication, and microbial improved oil recovery, produces microorganisms that result in a density gradient in a fluid. The bioconvection is caused by the erratically moving, more massive than liquid, motile microorganisms. Bacteria and microorganisms with dense stratification and thick coatings on top of the base fluid may become unstable because of unchecked expansion. Due to the motion, many bioconvection processes are investigated, including mixed convection, in which motile microorganisms initiate the flow network by transferring cells and oxygen from the top of the liquid to the bottom. Additionally, mixed convection and other management methods make use of these bacteria. They are used in biotechnology, biofuels, biosensor enzymes, fertilizers, and biomass. For many investigators, the bioconvection difficulties for the suspension of solid particles was a hot topic. Bioconvection is the mechanism through which suspensions of living microorganisms that are heavier than water, swim upward. Bioconvection describes the random movement of bacteria in single-celled or even

occasionally colony-like arrangements. The buoyancy of the fluid dramatically rises because of the gyrotactic bacteria upstream. Rao et al. [26] investigated the heat and mass transfer rates for the time-independent hydrodynamic bioconvection in a standard nanofluid flow. Raees et al. [27] gave the example in connection with mass and heat transport in gravity-driven bioconvection.

Narsimulu et al. [28] investigated the numerical method to MHD Carreau fluid channel in order to enable bulk bioconvection transmission across a non-linear expanding region. Koriko et al. [29] generated a stream of bioconvection on MHD nanoliquids via a vertical channel using nano entities and gyrotactic bacteria. In MHD bioconvection, Ferdows et al.'s [30] use of a considerably flexible sheet increased the thermal transfer of the nanofluid and stream. The bioconvection of oxytactic bacteria in a porous square cage was inspected by Balla et al. [31] using thermal radiation. Using heat radiation and Cattaneo-Christov flux, Mubaddel et al. [32] investigated Sisko nanoliquid bioconvection flow. They noticed a higher nanoliquid temperature as a result of a stronger Biot number. Palwasha et al. [33] described an analysis that considered the gravity-driven nanofluid stream made up of gyrotactic bacteria and nanomaterials. The heat and mass transfer theory of the time-dependent Williamson nanofluid flow of the magnetohydrodynamic (MHD) flow of gyrotactic motile microorganisms was investigated by Waqas et al. [34]. In a T-shaped cavity, the thermal performances of a liquid-based hybrid nanofluid were numerically reported by Almeshaal et al. [35]. A growing surface's Carreau nanofluid bioconvection flow was investigated by Shehzad et al. [36]. The bioconvection of oxytactic bacteria in a porous square cage was inspected by Balla et al. [37] with the help of thermal radiation.

2. MATHEMATICAL FORMULATION

Consider the flow of 2-D Maxwell reactive nanofluid with motile microorganism over stretching sheet. The energy equation contains thermal energy, which is obtained from Rosseland's approximation and saturation of the fluid done by Darcy-Forchheimer modal. The process of chemical reaction, Brownian diffusion and thermophoresis in porous medium are to be assumed. The magnetic field induction is discharged by a small Reynold's number, and it affects the flow with the help of momentum equation. There is no flow along the y-axis, only to be considered in the

orientation of x-axis. At the surface T_w and C_w are the wall conditions of temperature and concentration respectively. Whereas at the free surface, T_∞ and C_∞ are the ambient conditions. The physical representation is given by figure.

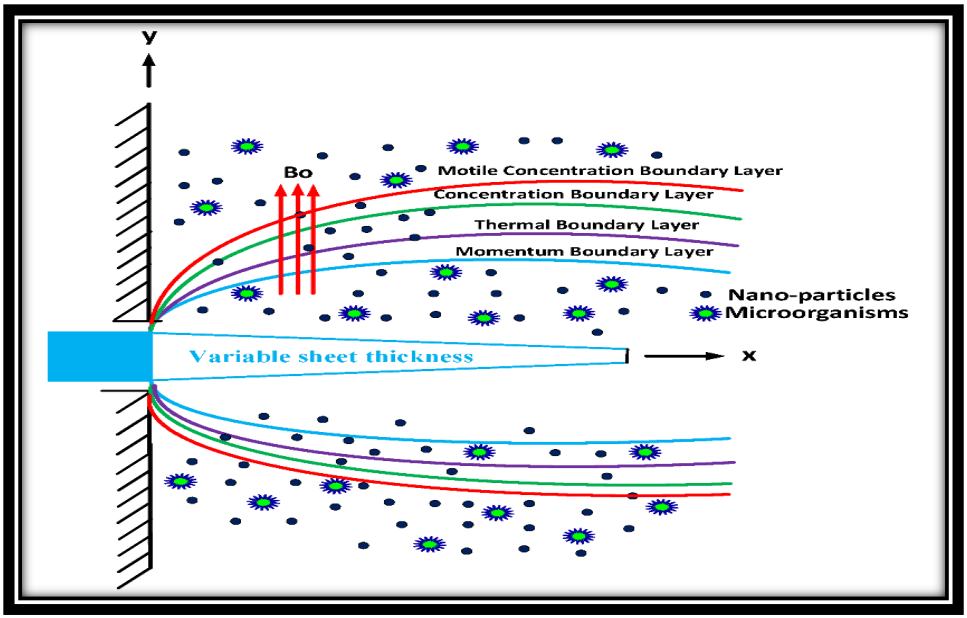

Figure 1. Geometry of Problem

The following describes the mathematical modeling of the temperature, concentration, momentum, continuity, and motile microbe equations under boundary layer assumptions:

2.1. Continuity Equation

$$\frac{\partial u}{\partial x}+\frac{\partial v}{\partial y}=0. \tag{1}$$

2.2. Momentum Equation

$$u\frac{\partial u}{\partial x}+v\frac{\partial u}{\partial y}+\delta_0\left(u^2\frac{\partial}{\partial x}\left(\frac{\partial u}{\partial x}\right)+v^2\frac{\partial}{\partial y}\left(\frac{\partial u}{\partial y}\right)+2vu\frac{\partial}{\partial x}\left(\frac{\partial u}{\partial y}\right)\right)=\upsilon\frac{\partial}{\partial y}\left(\frac{\partial u}{\partial y}\right)$$
$$-\frac{\sigma B_0^2 u}{\rho}-\frac{\sigma\delta_0 B_0^2}{\rho}\left(v\frac{\partial u}{\partial y}\right)-\left(\frac{\upsilon}{K_1}+\frac{C_b}{x\sqrt{K_1}}u\right)u+\frac{1}{\rho_l}\begin{bmatrix}(1-C_l)\rho_l\beta^{**}\kappa(T-T_\infty)\\-(\rho_P-\rho_l)\kappa(C-C_\infty)\\-(N-N_\infty)\kappa\gamma(\rho_m-\rho_l)\end{bmatrix}. \tag{2}$$

2.3. Energy Equation

$$u\frac{\partial T}{\partial x}+v\frac{\partial T}{\partial y}=\varpi\frac{\partial}{\partial y}\left(\frac{\partial T}{\partial y}\right)+\frac{\tau \mathrm{B}}{\delta_C}\frac{\partial T}{\partial y}\frac{\partial C}{\partial y}+\frac{\tau D_T}{T_\infty}\left(\frac{\partial T}{\partial y}\right)^2 -\frac{1}{\rho c}\frac{\partial Q}{\partial y}+\frac{Q_0}{(\rho c_p)_l}(T_\infty-T_0)\exp\left(-\sqrt{\frac{a}{v_l}}ny\right). \tag{3}$$

2.4. Concentration Equation

$$u\frac{\partial C}{\partial x}+v\frac{\partial C}{\partial y}=\mathrm{B}\frac{\partial}{\partial y}\left(\frac{\partial C}{\partial y}\right)+\frac{\delta_C D_T}{T_\infty}\frac{\partial}{\partial y}\left(\frac{\partial T}{\partial y}\right)-Cr(C-C_\infty)\ . \tag{4}$$

2.5. Motile Microorganism's Equation:

$$u\frac{\partial N}{\partial x}+v\frac{\partial N}{\partial y}+\frac{b\mathrm{E}}{(C_w-C_\infty)}\left[\frac{\partial}{\partial y}\left(N\frac{\partial C}{\partial y}\right)\right]=D_m\frac{\partial^2 N}{\partial y^2}. \tag{5}$$

2.6. Boundaries Conditions

$$u=U_w=ex, k\frac{\partial T}{\partial y}=-h_l(T_s-T), \mathrm{B}\frac{\partial C}{\partial y}=-h_s(C_s-C),$$

$$N=N_w \quad at \quad y=0. \tag{6}$$

$$u\to 0,\ T\to T_\infty,\ C\to C_\infty,\ N\to N_\infty\ as\ y\to\infty. \tag{7}$$

The radiative heat flow derived from Rosseland's estimate is displayed by the number Q in equation (3).

Mathematically,

$$Q=-\frac{4\sigma_{SB}}{3K_{abs}}\frac{\partial T^4}{\partial y}. \tag{8}$$

Where σ_{SB} is the Stefan-Boltzmann constant and K_{abs} is the mean absorption constant.

By expansion of Taylor series on T^4 and ignoring the more than one order terms in $(T-T_\infty)$, we have

$$\frac{\partial Q}{\partial y}=-\frac{16}{3}\frac{\sigma_{SB}T_B^3}{K_{abs}}\left(\frac{\partial^2 T}{\partial y^2}\right). \tag{9}$$

Then equation (3) becomes as:

$$u\frac{\partial T}{\partial x}+v\frac{\partial T}{\partial y}=\varpi\frac{\partial}{\partial y}\left(\frac{\partial T}{\partial y}\right)+\frac{\tau \mathrm{B}}{\delta_C}\frac{\partial T}{\partial y}\frac{\partial C}{\partial y}+\frac{\tau D_T}{T_\infty}\left(\frac{\partial T}{\partial y}\right)^2+\frac{16}{3(\rho c)}\frac{\sigma_{BC}T_\infty^3}{K_{abs}}\frac{\partial^2 T}{\partial y^2} +\frac{Q_0}{(\rho c_p)_l}(T_\infty-T_0)\exp\left(-\sqrt{\frac{a}{v_l}}ny\right). \tag{10}$$

2.7. Similarity Variables

The similarity variables for governing equations described as

$$u = exf'(\eta),\ \theta(\eta) = \frac{(T - T_\infty)}{(T_w - T_\infty)},\ \phi(\eta) = \frac{(C - C_\infty)}{(C_w - C_\infty)},\ v = -(ev)^{1/2} f(\eta),$$
$$\eta = \sqrt{\frac{e}{v}}y,\ \chi(\zeta) = \frac{N - N_\infty}{N_w - N_\infty},\ \zeta = \sqrt{\frac{e}{v}}y.$$

Using similarity variables and all of its required derivatives values in Equations (2) - (10), we will get

$$f''' + (1 + M^2\psi)ff'' + 2\psi ff'f'' - \psi f^2 f''' - (\lambda + M^2)f' - (F_r + 1)f'^2 + \Lambda(\theta - Nr\phi - Nc\chi) = 0. \quad (11)$$

$$\left(1 + \frac{4}{3}Rd\right)\theta'' = Prf\theta' + PrN_b\theta'\phi' + PrN_t\theta'^2 + Pr\delta e^{-n\eta}. \quad (12)$$

$$\phi'' + PrLef\phi' + \frac{N_t}{N_b}\theta'' - K\phi = 0. \quad (13)$$

$$\chi'' + Lbf\chi' - Pe[\phi''(\chi + \delta_1) + \chi'\phi'] = 0. \quad (14)$$

With

$$f(0) = 0,\ f'(0) = 1,\ \theta(0) = 1,\ \phi(0) = 1,\ \chi(0) = 1,$$
$$f'(\infty) \to 0,\ \theta(\infty) \to 0,\ \phi(\infty) \to 0,\ \chi(\infty) \to 0.$$

Where

$$M^2 = \frac{\sigma B_0^2}{e\rho},\ \psi = \delta e,\ \lambda = \frac{v}{eK_1},\ F_r = \frac{C_b}{\sqrt{K_1}},\ \Lambda = \frac{(1 - C_l)\beta^{**}\kappa(T_w - T_\infty)}{e^2 x},$$
$$Nr = \frac{(\rho_p - \rho_l)(C_w - C_\infty)}{\beta^{**}\rho_l(1 - C_l)(T_w - T_\infty)},\ Nc = \frac{(\rho_m - \rho_l)\gamma(N_w - N_\infty)}{\beta^{**}\rho_l(1 - C_l)(T_w - T_\infty)}.$$

$$Rd = \frac{4}{(\rho C)}\frac{\sigma_{SB}T_\infty^3}{\delta K_{abs}},\ N_b = \frac{\tau \mathrm{B}}{v\delta_C}(C_w - C_\infty),\ N_t = \frac{\tau D_T}{vT_\infty}(T_w - T_\infty),\ \delta = \frac{Q_0}{e(\rho C_P)_l}\frac{(T_\infty - T_0)}{(T_w - T_\infty)}.$$

$$Pr = \frac{v}{\varpi},\ Le = \frac{\varpi}{\mathrm{B}},\ N_t = \tau D_T\frac{(T_w - T_\infty)}{vT_\infty},\ N_b = \tau \mathrm{B}\frac{(C_w - C_\infty)}{v\delta_C},\ K = \frac{Cr}{e}.$$

$$Lb = \frac{\upsilon}{D_m}, Pe = \frac{b\mathrm{E}}{D_m}, \delta_1 = \frac{N_\infty}{N_w - N_\infty}.$$

Here, λ is the porosity parameter, F_r is the local inertia, Λ is the mixed convection parameter, Nr is the buoyancy ratio parameter, Nc is the bioconvection Rayleigh parameter, Rd is the radiation factor, Pr is the prandtl factor, N_b is the Brownian diffusion parameter, N_t is the thermophoretic parameter, B is the Brownian diffusion factor, K is the first order chemical reaction, δ_1 is the bioconvection, Lb represent the bioconvection Lewis number and Pe is the Peclet number.

3. NUMERICAL SCHEME

The computational tool MATLAB bvp4c is used to solve the current problem. In comparison to numerical approaches, it is further difficult to find results to nonlinear differential equations using numerous physical techniques. There are several methods that may be used to get the answer to a challenging nonlinear equation, but the shooting method is the simplest. Shooting methods also make the issue of relative boundary limits easier to solve. A well-known shooting technique called bvp4c is used in MATLAB, when handling odd flow characteristics. The first-order ODEs are subjected to the bvp4c method. We must have to convert connected dimensionless differential equations with boundary conditions into a system of first-order simultaneous equations in order to generate bvp4c.

Consider

$f = q_0, \quad f' = q_1, \quad f'' = q_2, \quad f''' = q'_2, \theta = q_3, \quad \theta' = q_4, \quad \theta'' = q'_4, \phi = q_5, \quad \phi' = q_6, \quad \phi'' = q'_6,$

$\chi = q_7, \quad \chi' = q_8, \quad \chi'' = q'_8,$

Using above expressions in (11), (12), (13) and (14), we will get

$$q'_2 = \frac{1}{(1-M^2\gamma)}\left[(\lambda+M^2)q_1+(F_r+1)q_1^2-(1+M^2\gamma)q_0q_2-2\gamma q_0q_1q_2-\Lambda(q_3-Nrq_5-Ncq_7)\right]$$

$$q'_4 = -\frac{Pr}{\left(1+\frac{4}{3}Rd\right)}\left[q_0q_4+N_bq_4q_6+N_tq_4^2\right]$$

$$q'_6 = Kq_5-PrLeq_0q_6-\frac{N_t}{N_b}q'_4$$

$$q'_8 = Pe\left[q'_6(q_7+\delta_1)+q_8q_6\right]-Lbq_0q_8$$

with

$$q_0(0) = 0, \quad q_1(0) = 1, \quad q_3(0) = 1, \quad q_5(0) = 1, \quad q_7(0) = 1,$$

$$q_1(\infty) \to 0, \quad q_3(0) \to 0, \quad q_5(\infty) \to 0, \quad q_7(\infty) \to 0,$$

4. DISCUSSION

Using basic boundary conditions and the influence of Darcy-Forchheimer and Lorentz forces, we investigated the effects of an exponential space-based internal heat source on bio-convective maxwell nanofluid flow caused by an extended sheet. In this section, special effects of different flow adjusting parameters compared to velocity field, thermal field, concentrations of nanoparticles and microorganism density field are presented. The velocity's performance for the variation in the buoyancy ratio number, Deborah number, bio-convection Rayleigh parameter, magnetic parameter, porosity parameter, and local inertia is shown in Figures 2-7.

Figure 2 describes the impacts of buoyancy ratio parameter versus velocity field. It is shown that increased buoyancy ratio parameter values result in decreased velocity because thermal convection is weakened when solutal buoyancy is opposed, which raises resistance and slows fluid velocity. Figure 3 inspects the influence of bioconvection Rayleigh number via velocity of nanofluid flow. Higher levels of the bioconvection Rayleigh number are seen to decrease the velocity field due to the thickening of the viscous layer. Density stratification is improved, and main convection is resisted by stronger microbe buoyancy. Figure 4 shows the velocity field's activities in relation to the magnetic parameter. From the results we concluded that for larger values of magnetic parameter, velocity is declined because of stronger Lorentz force opposing flow motion, dissipating energy, and increasing resistance. The relationship between the velocity field and the mixed convection parameter is examined in Figure 5. In this case, when the mixed convection parameter rises, the nanofluid's velocity field rises up. Figure 6 explained the behavior of velocity field versus local inertia parameter. From the velocity curves we determined that velocity field lessens via escalating the magnitude of local inertia parameter. As the Deborah number increases, Figure 7 shows that the velocity field decreases.

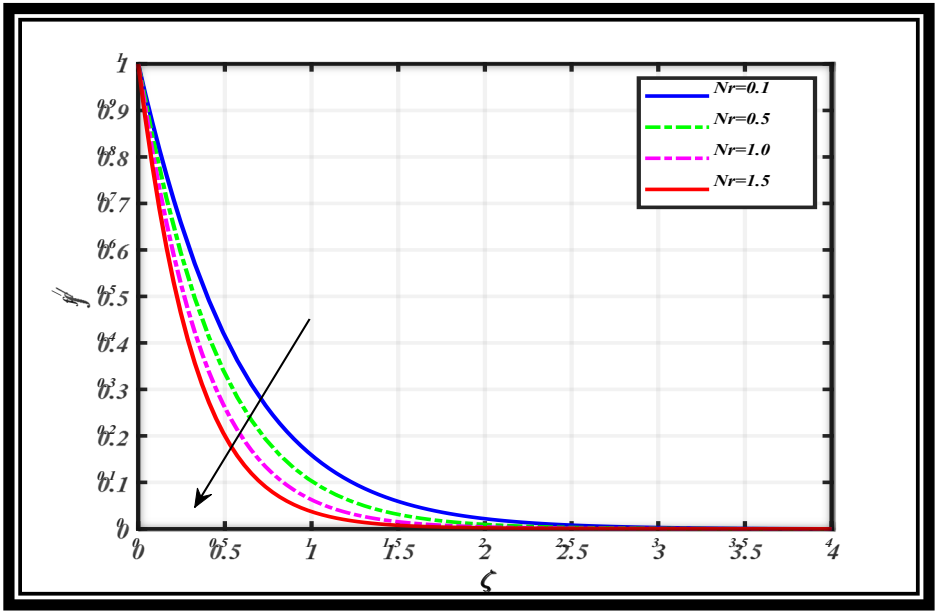

Figure 2. Relationship between Nr and f'

In order to observe the effect of radiation factor, exponential space-based heat source, the Prandtl number, Brownian diffusion parameter, Magnetic parameter and Local inertia on the temperature field as shown in Figures 8-13. The purpose of Figure 8 is to show how the thermal radiation parameter affects the species' thermal field. It has been shown that the velocity field improves as the thermal radiation parameter values escalate. The reason behind is that radiation increases temperature and buoyancy, reduces viscosity, and strengthens convective motion. Figure 9 illustrates the inspiration of the exponential space base heat source parameter vs temperature distribution. From the curve lines, it is detected that temperature distribution is reduced for higher exponential space base heat source parameter because heat generation decays more quickly in space, decreasing total heat energy and cooling the fluid field. The influence of the Brownian motion parameter and Prandtl number on the thermal field is seen in Figures 10 and 11. Here the thermal field is lessened for Prandtl number, but inverse trend is noticed for Brownian motion parameter. The relationship between the local inertia and magnetic parameters on the thermal field are depicted in Figures 12 and 13. It has been noted that when the values of the local inertia and magnetic parameters increase, so does the heat field.

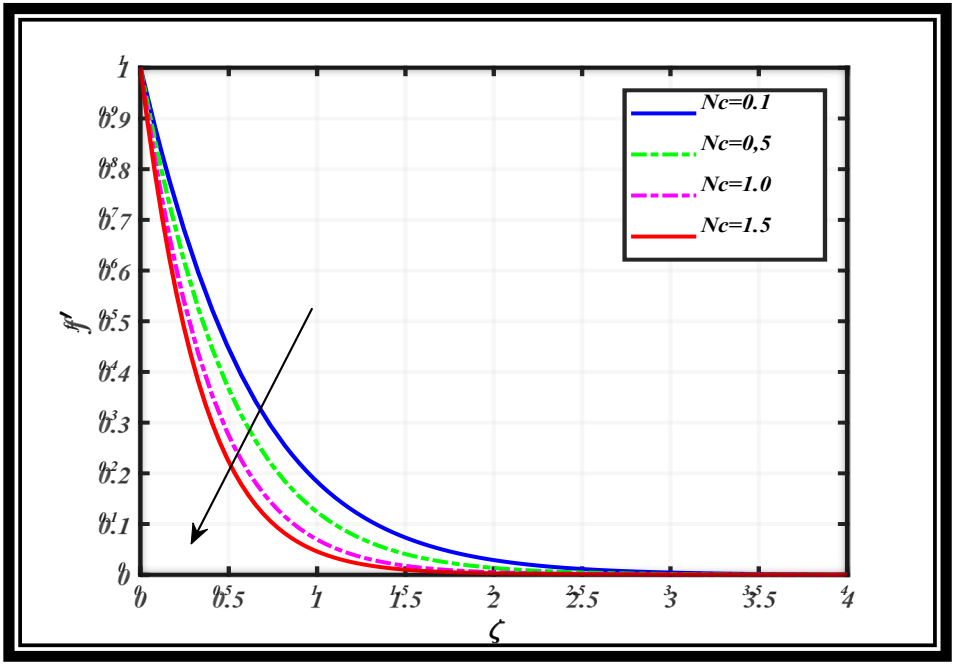

Figure 3. Relationship between Nc and f'

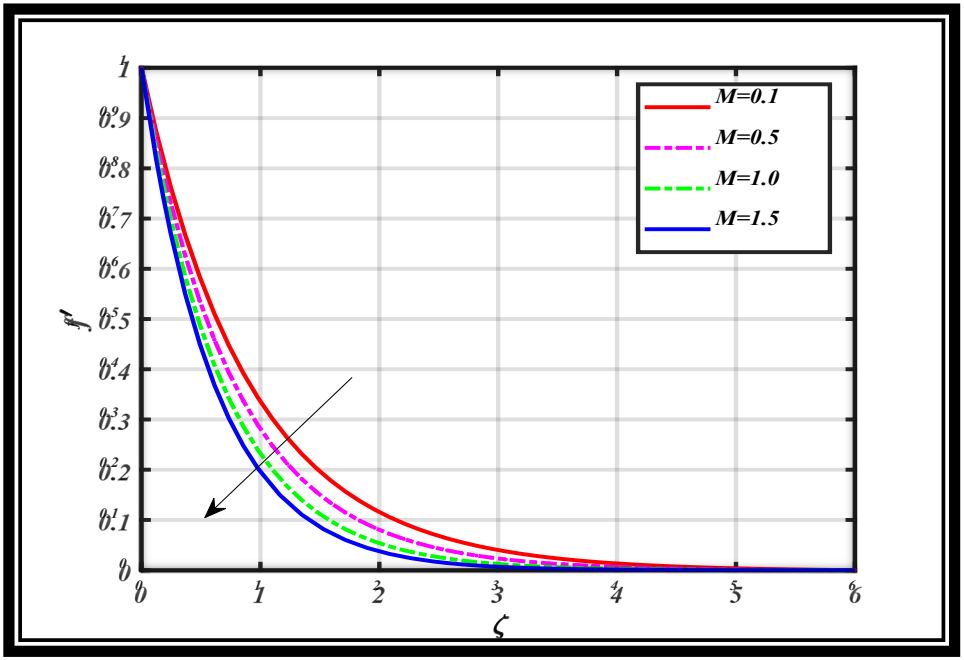

Figure 4. Relationship between M and f'.

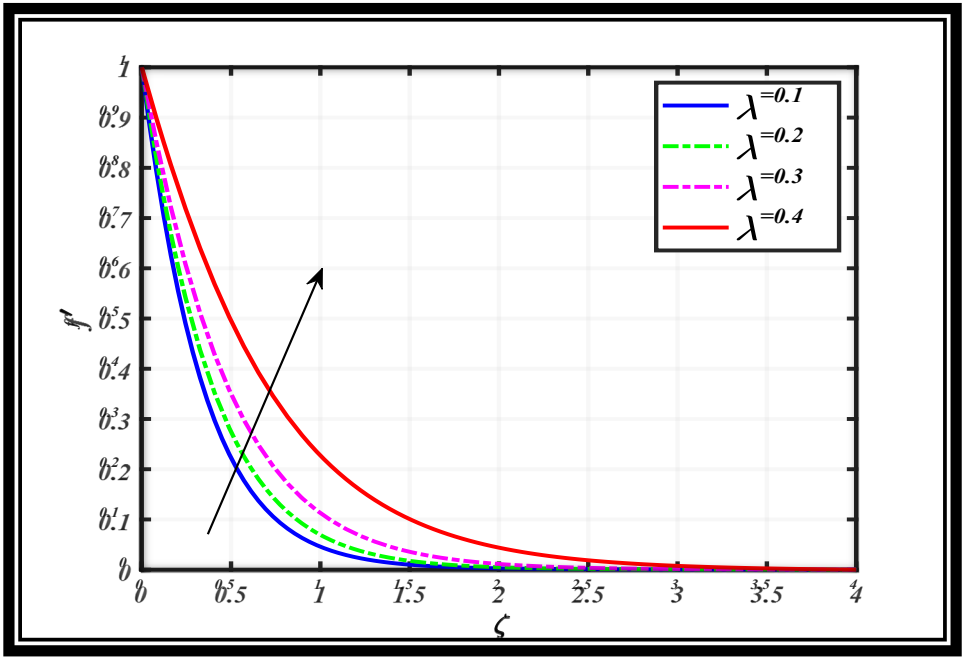

Figure 5. Relationship between λ and f'.

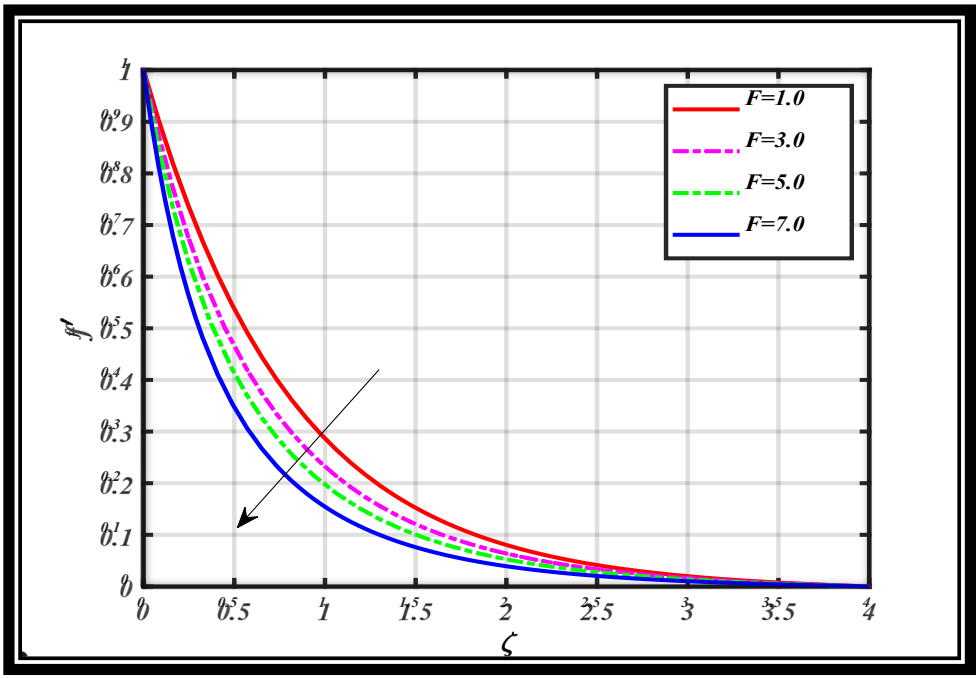

Figure 6. Relationship between F and f'.

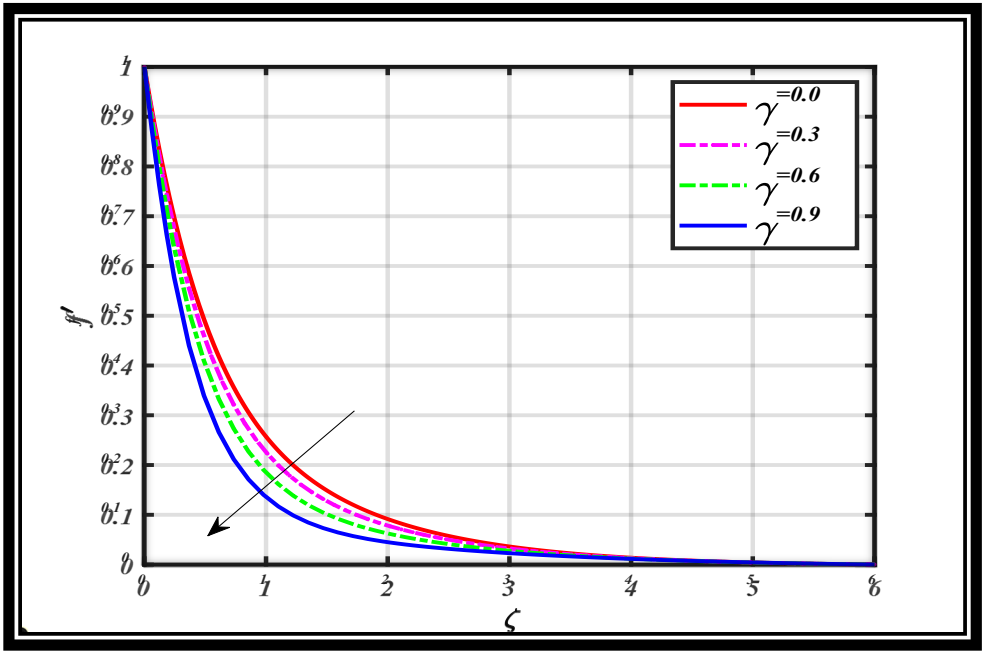

Figure 7. Relationship between γ and f'.

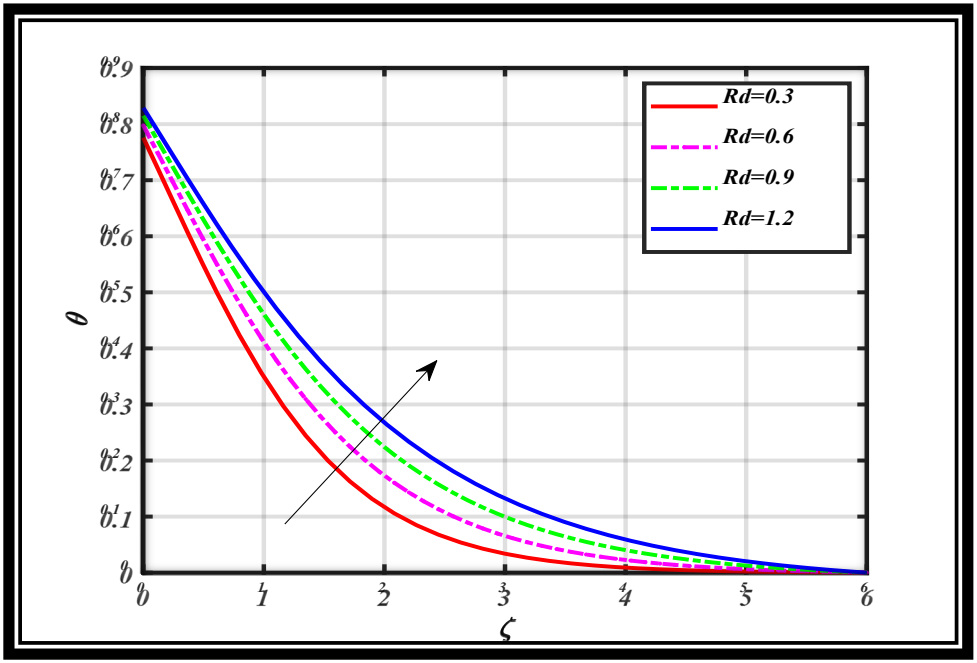

Figure 8. Relationship between Rd and θ.

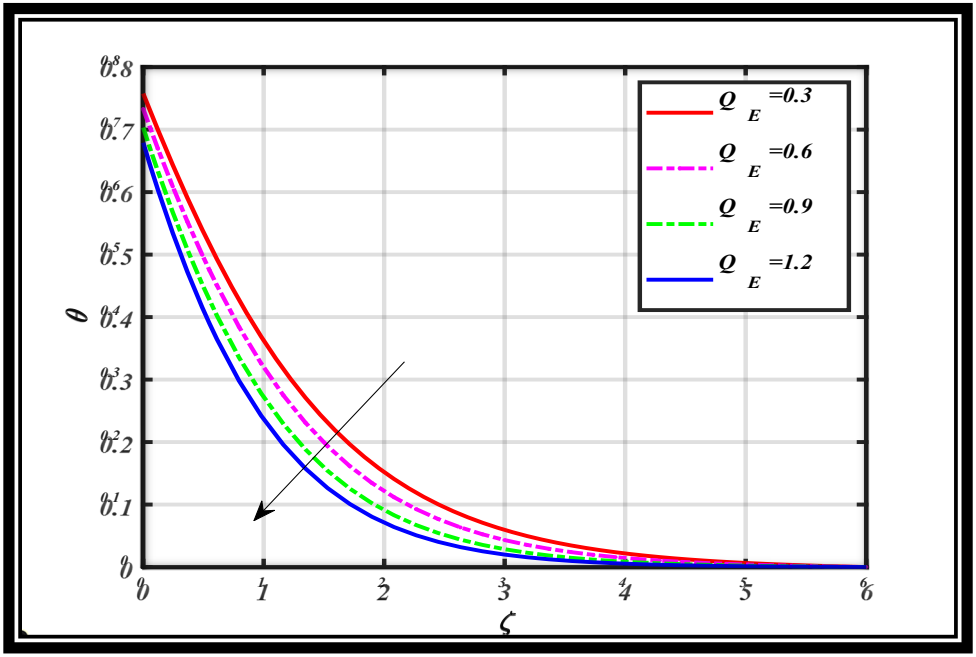

Figure 9. Relationship between Q_E and θ.

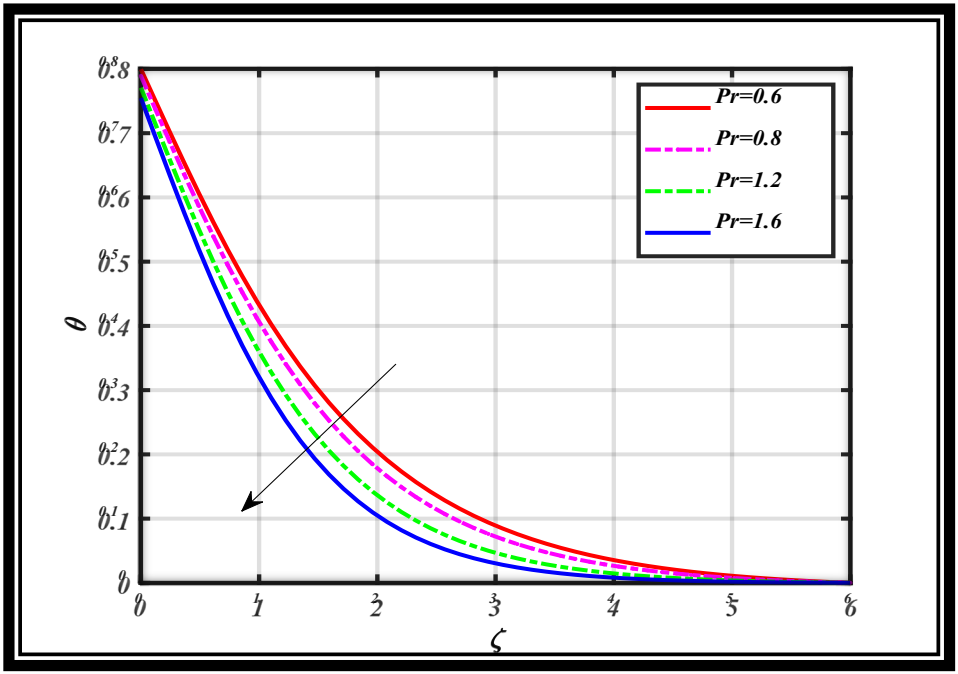

Figure 10. Relationship between Pr and θ.

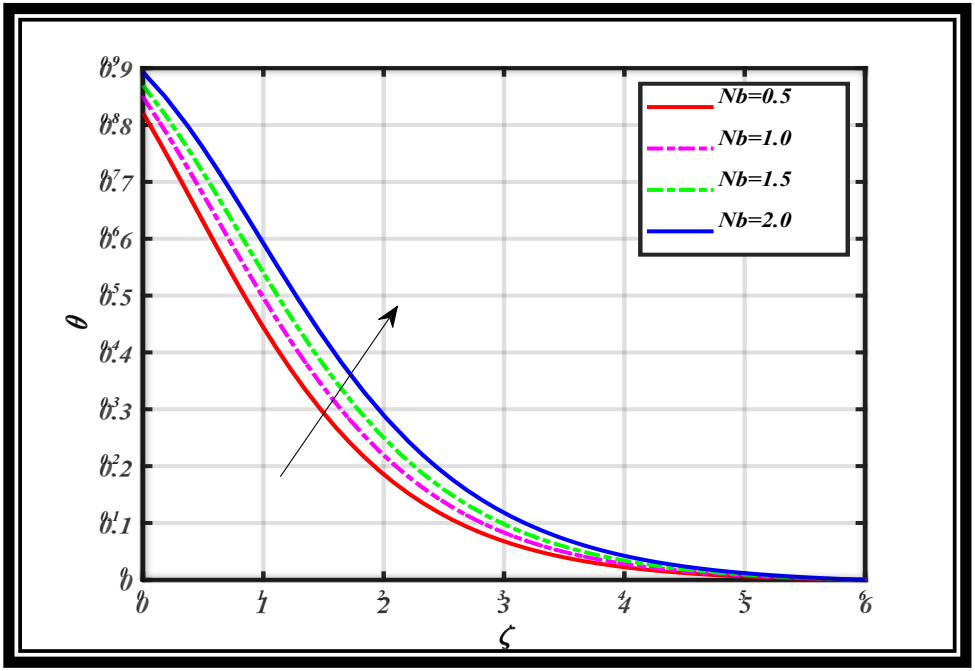

Figure 11. Relationship between Nb and θ.

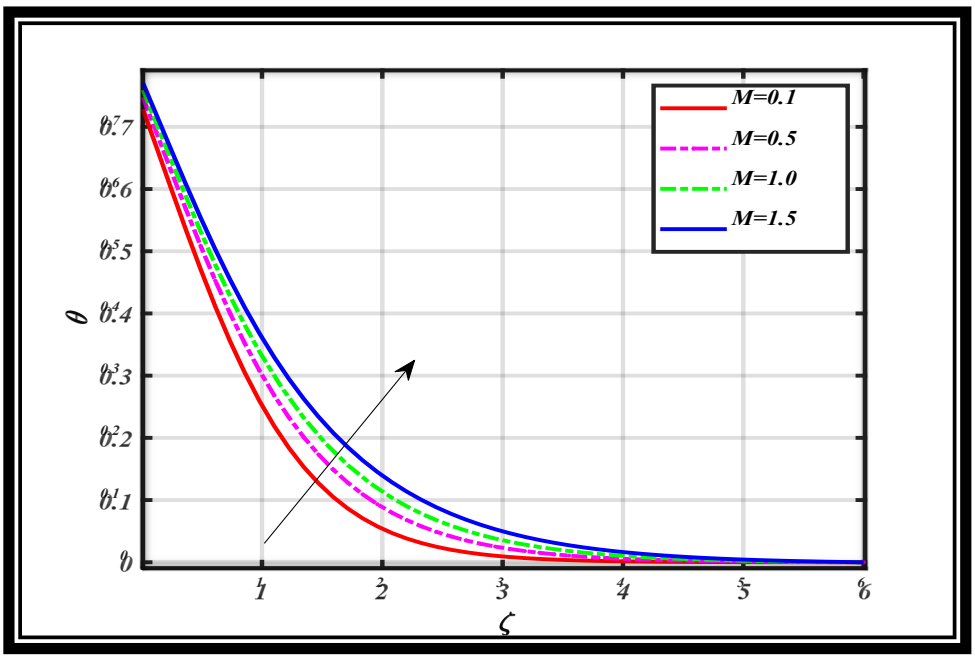

Figure 12. Relationship between M and θ.

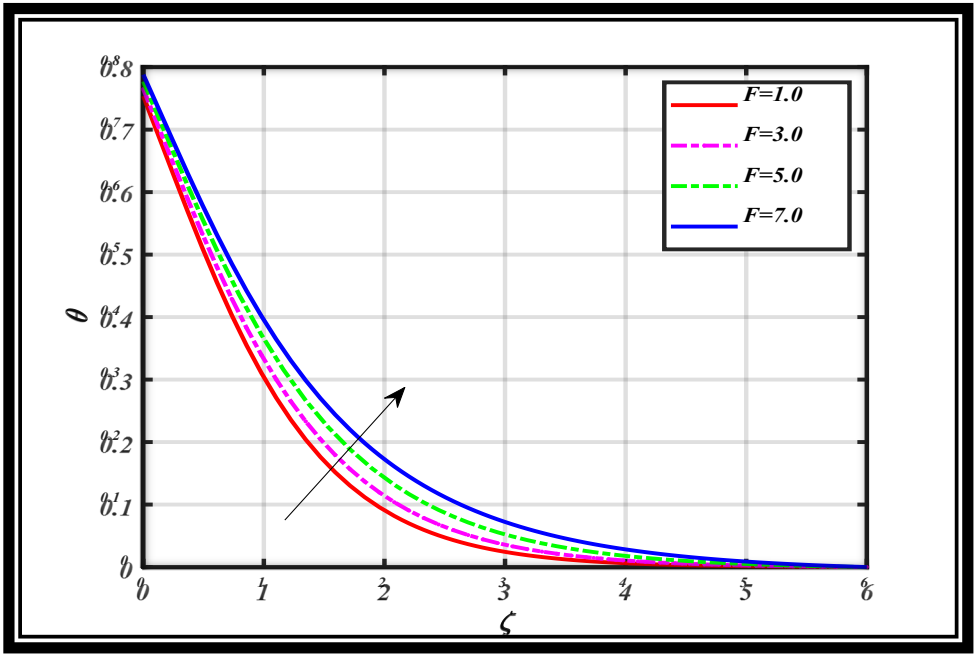

Figure 13. Relationship between F and θ.

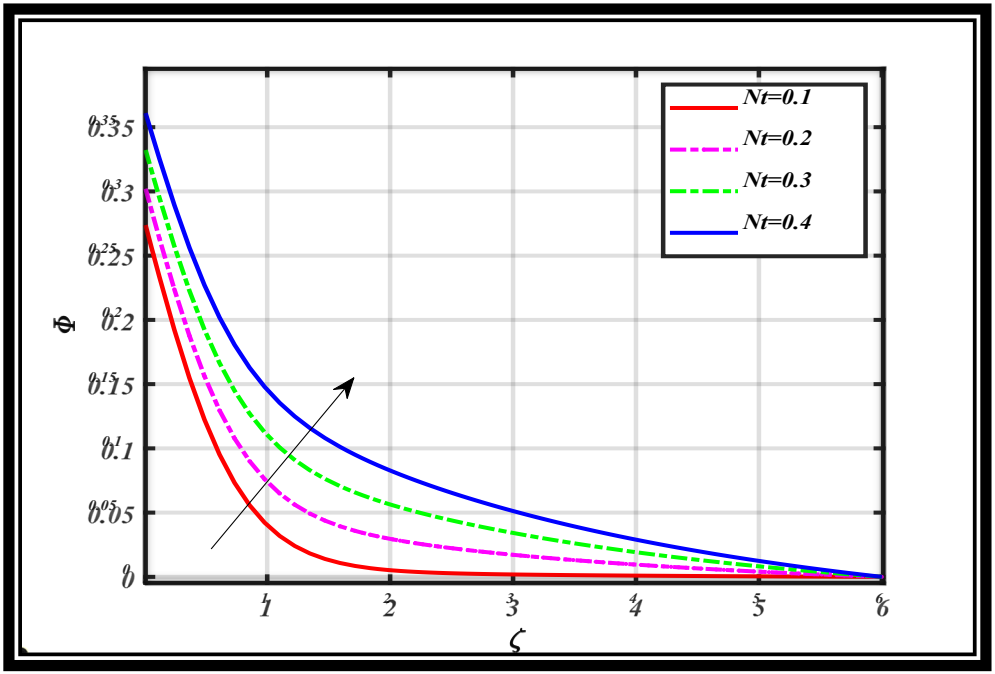

Figure 14. Relationship between Nt and Φ.

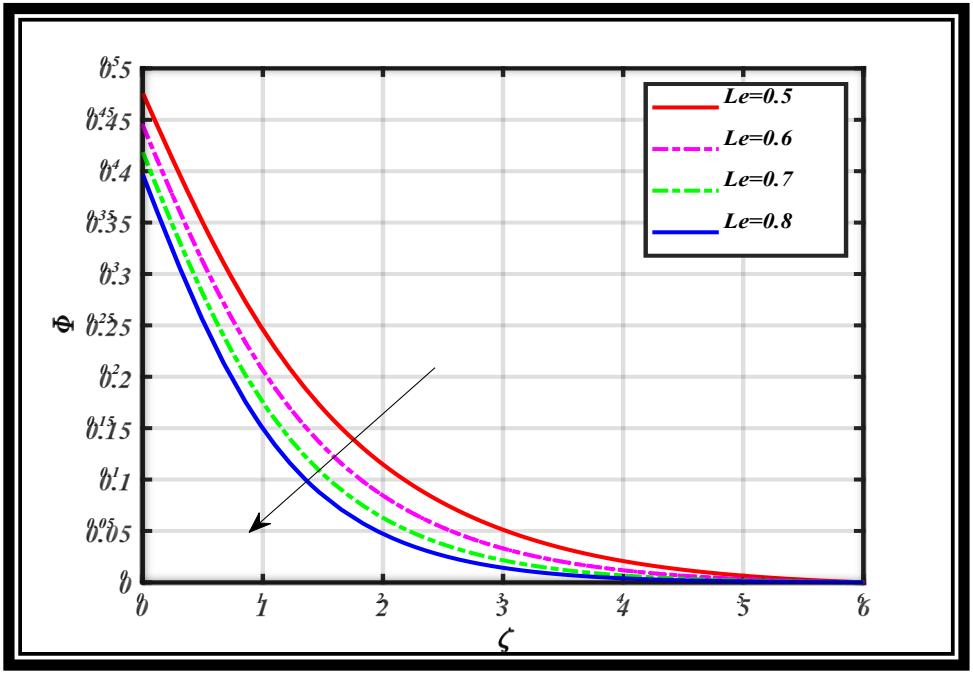

Figure 15. Relationship between Le and Φ.

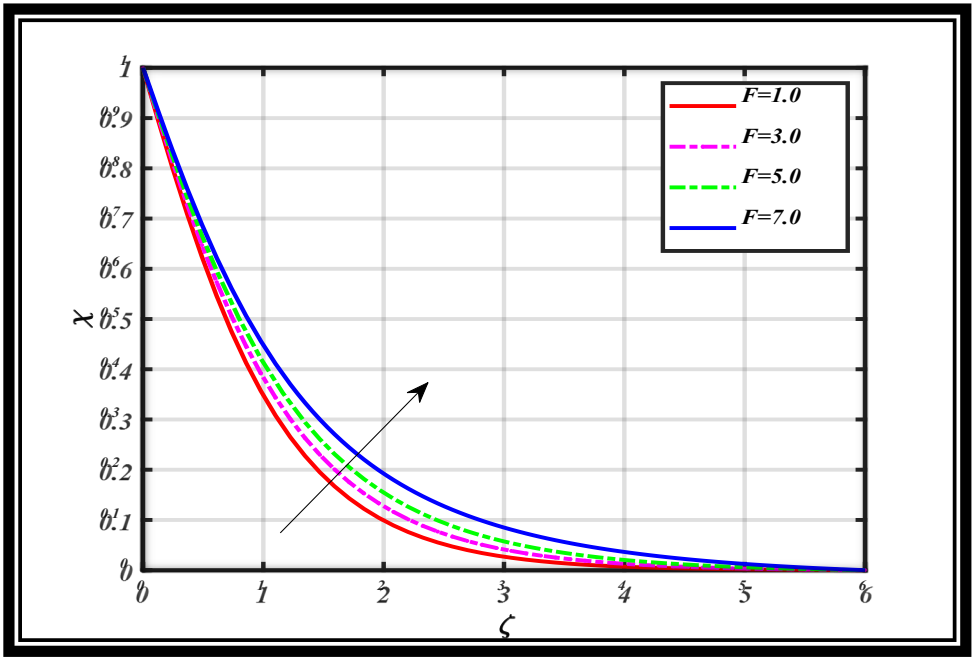

Figure 16. Relationship between F and χ.

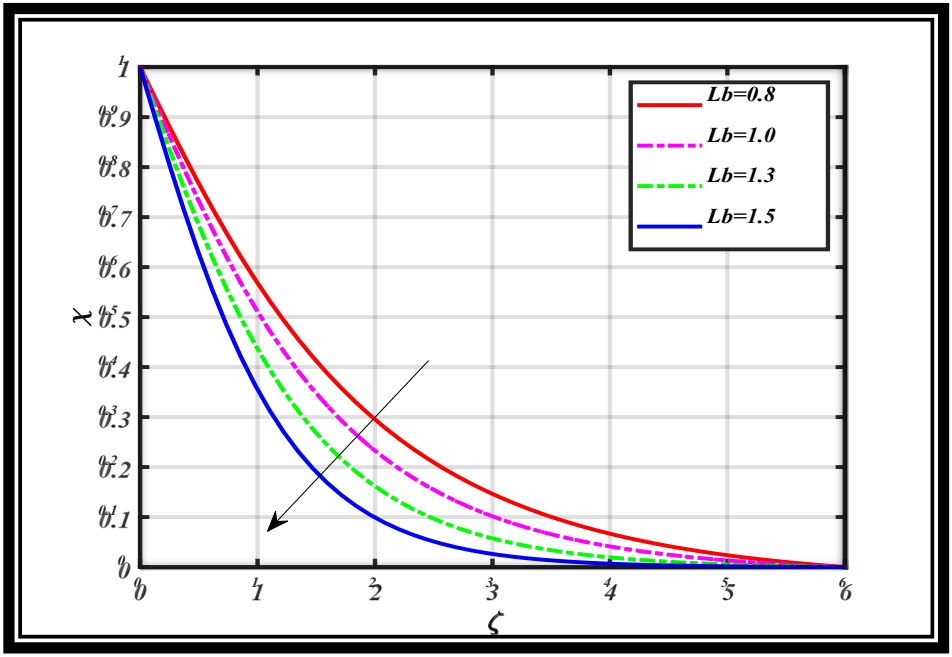

Figure 17. Relationship between Lb and χ.

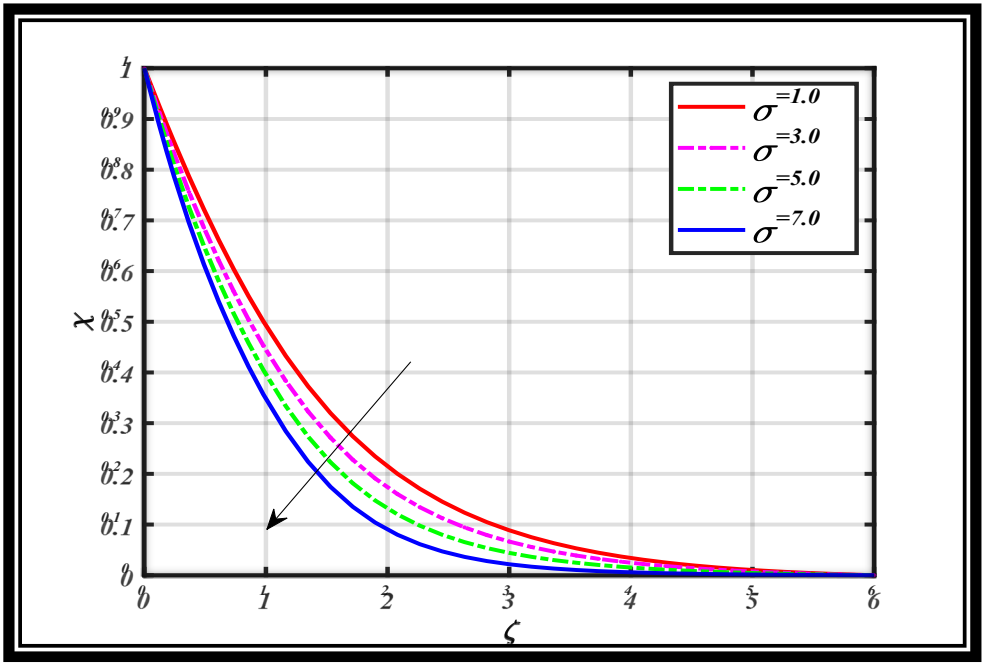

Figure 18. Relationship between σ and χ.

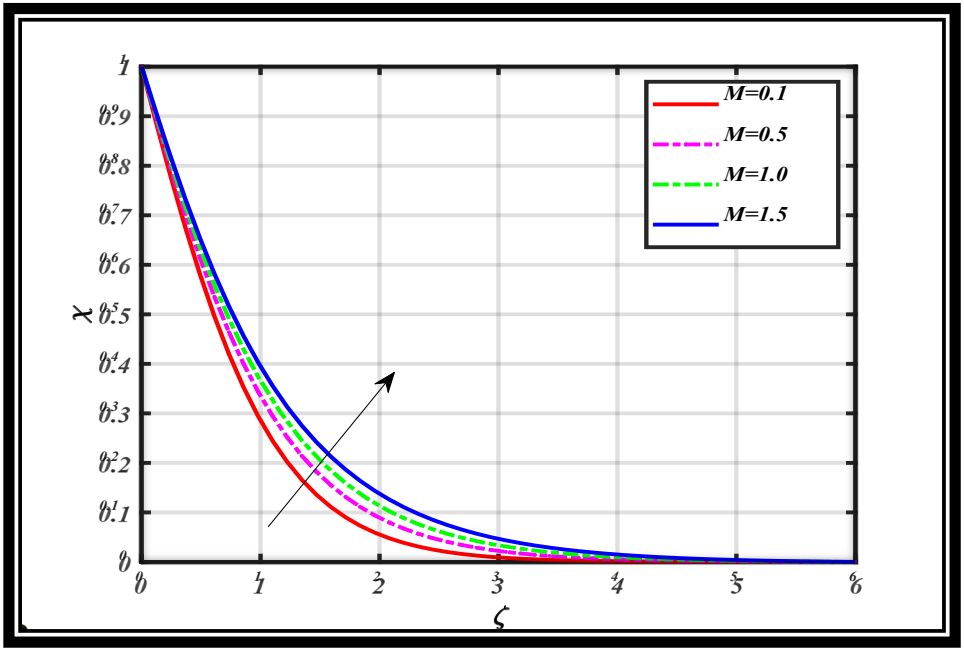

Figure 19. Relationship between M and χ .

Figures 14–15 illustrate how the concentration field is affected by the Lewis number and thermophoresis parameter. Figure 14 illustrates how the concentration field of the nanoparticle is affected by the thermophoresis parameter. As the values of that parameter climb, so does the fluid's concentration. As seen in figure 15, the graph shows a declining trend in the concentration profile as a result of higher Lewis factor values due to reduced mass diffusivity, limiting nanoparticle transport, thinning the concentration boundary layer.

The purpose of Figure 16 is to evaluate how the microorganism density field is affected by the local inertia value. As the local inertia parameter values accumulate, the microbe field increases. The purpose of Figure 17 is to show how the microorganism density field and the bioconvection Lewis number interact. This represents a higher bioconvection Lewis number, decreasing the field of microorganisms. Figure 18 illustrates the behavior of microorganism's difference parameter versus microorganism density field. It is examined that microorganism density field is reduced via larger microorganism's difference parameter due to declined microorganism diffusivity and enhanced convective transport, leading to thinner microorganism boundary layer. Figure 19 indicates the impact of magnetic

parameter on microorganism density field. From the curves lines it is concluded that microorganism density field is improved for higher magnetic parameter due to Lorentz force slowing fluid motion, allowing microorganisms to accumulate and stabilize in the bioconvective region.

4.1. Conclusion

An increment in magnetic parameter depicts a decreasing behavior of velocity profile. Velocity field is declined for buoyancy ratio parameter and bioconvection Rayleigh number. The velocity field is lessened via higher values of Deborah number. As the inertia parameter values increase, the velocity drops. The impact of Prandtl number causes a decrease in temperature distribution. For escalating amounts of magnetic parameter and thermophoresis, the temperature field improves. Higher amount of thermal Biot number and Radiation parameter increased the temperature of fluid. The concentration of nanoparticles rises as the thermophoresis parameter values rise. The bioconvection Lewis number decreases in the microorganism's field as the Peclet number rises.

Author Contribution

Muhammad Arbaz: conceptualization, validation, visualization, writing – original draft, writing – review & editing. **Muhammad Khurshid Azam:** project administration, formal analysis, investigation

Muhammad Imran: supervision, resources, software, methodology

Conflicts of Interest

The authors of the manuscript have no financial or non-financial conflict of interest in the subject matter or materials discussed in this manuscript.

Data Availability Statement

The data associated with the study will be provided by the corresponding author if requested

Funding Details

This research received no external funding**.**

Generative AI Disclosure Statement

The authors did not used any type of generative artificial intelligence software for this research.

REFERENCES

1. Akinshilo AT, Davodi A, Ilegbusi A, Sobamowo G. Thermal analysis of radiating film flow of sodium alginate using MWCNT nanoparticles. *J Appl Comp Mech*. 2022;8(1):219-231. https://doi.org/10.22055/jacm.2020.33386.2218

2. Jakati SV, Nargund AL, Sathyanarayana SB. Study of Maxwell nanofluid flow over a stretching sheet with non-uniform heat source/sink with external magnetic field. *J Adv Res Fluid Mech Therm Sci*. 2019;55(2):218-232.
3. Yusuf TA, Mabood F, Prasannakumara BC, Sarris IE. Magneto-bioconvection flow of Williamson nanofluid over an inclined plate with gyrotactic microorganisms and entropy generation. *Fluids*. 2021;6(3):e109. https://doi.org/10.3390/fluids6030109
4. Hady FM, Ibrahim FS, Abdel-Gaied SM, Eid MR. Radiation effect on viscous flow of a nanofluid and heat transfer over a nonlinearly stretching sheet. *Nanoscale Res Lett*. 2012;7(1):e229. https://doi.org/10.1186/1556-276X-7-229
5. Souayeh B, Kumar KG, Reddy MG, et al. Slip flow and radiative heat transfer behavior of titanium alloy and ferromagnetic nanoparticles along with suspension of dusty fluid. *J Mol Liq*. 2019;290:e111223. https://doi.org/10.1016/j.molliq.2019.111223
6. Ahmed J, Khan M, Ahmad L. Radiative heat flux effect in flow of Maxwell nanofluid over a spiraling disk with chemically reaction. *Phys A*. 2020;551:e123948. https://doi.org/10.1016/j.physa.2019.123948
7. Farooq U, Lu D, Munir S, Ramzan M, Suleman M, Hussain S. MHD flow of Maxwell fluid with nanomaterials due to an exponentially stretching surface. *Sci Rep*. 2019;9(1):e7312. https://doi.org/10.1038/s41598-019-43549-0
8. Mahmood M, Asghar S, Hossain MA. Squeezed flow and heat transfer over a porous surface for viscous fluid. *Heat Mass Transfer*. 2007;44(2):165-173. https://doi.org/10.1007/s00231-006-0218-3
9. Pedley TJ, Hill NA, Kessler JO. The growth of bioconvection patterns in a uniform suspension of gyrotactic micro-organisms. *J Fluid Mech*. 1988;195:223-237. https://doi.org/10.1017/s0022112088002393
10. Rashad AM, Chamkha AJ, Modather M. Mixed convection boundary-layer flow past a horizontal circular cylinder embedded in a porous medium filled with a nanofluid under convective boundary condition. *Comput Fluids*. 2013;86:380-388. https://doi.org/10.1016/j.compfluid.2013.07.030
11. Zheng L, Zhang C, Zhang X, Zhang J. Flow and radiation heat transfer of a nanofluid over a stretching sheet with velocity slip and temperature jump in porous medium. *J Franklin Inst*. 2013;350(5):990-1007. https://doi.org/10.1016/j.jfranklin.2013.01.022

12. Aziz A, Alsaedi A, Muhammad T, Hayat T. Numerical study for heat generation/absorption in flow of nanofluid by a rotating disk. *Results Phys*. 2018;8:785-792. https://doi.org/10.1016/j.rinp.2018.01.009
13. Chu Y-M, Shankaralingappa BM, Gireesha BJ, Alzahrani F, Khan MI, Khan SU. RETRACTED: Combined impact of Cattaneo-Christov double diffusion and radiative heat flux on bio-convective flow of Maxwell liquid configured by a stretched nano-material surface. *Appl Math Comput*. 2022;419:e126883. https://doi.org/10.1016/j.amc.2021.126883
14. Zhang X-H, Shah R, Saleem S, Shah NA, Khan ZA, Chung JD. Natural convection flow maxwell fluids with generalized thermal transport and Newtonian heating. *Case Stud Therm Eng*. 2021;27:e101226. https://doi.org/10.1016/j.csite.2021.101226
15. Lund LA, Wakif A, Omar Z, Khan I, Animasaun IL. Dynamics of water conveying copper and alumina nanomaterials when viscous dissipation and thermal radiation are significant: single-phase model with multiple solutions. *Math Methods Appl Sci*. 2022:46(1):1603-1617. https://doi.org/10.1002/mma.8270
16. Wakif A, Boulahia Z, Ali F, Eid MR, Sehaqui R. Numerical analysis of the unsteady natural convection MHD Couette nanofluid flow in the presence of thermal radiation using single and two-phase nanofluid models for Cu–water nanofluids. *Int J Appl Comp Math*. 2018;4(3):1-27. https://doi.org/10.1007/s40819-018-0513-y
17. Sharma RP, Raju MC, Makinde OD, Reddy PRK, Reddy PC. Buoyancy effects on unsteady MHD chemically reacting and rotating fluid flow past a plate in a porous medium. *Defect Diffus Forum*. 2019;392:1-9. https://doi.org/10.4028/www.scientific.net/DDF.392.1
18. Shafiq A, Khan I, Rasool G, Seikh AH, Sherif E-S. Significance of double stratification in stagnation point flow of third-grade fluid towards a radiative stretching cylinder. *Mathematics*. 2019;7(11):e1103. https://doi.org/10.3390/math7111103
19. Abbas N, Nadeem S, Malik MY. Theoretical study of micropolar hybrid nanofluid over Riga channel with slip conditions. *Phys A*. 2020;551:e124083. https://doi.org/10.1016/j.physa.2019.124083
20. Kolsi L, Abidi A, Borjini MN, Daous N, Ben Aïssia H. Effect of an external magnetic field on the 3-D unsteady natural convection in a cubical enclosure. *Numer Heat Transf A*. 2007;51(10):1003-1021. https://doi.org/10.1080/10407790601184462

21. Sheikholeslami M, Rokni HB. Simulation of nanofluid heat transfer in presence of magnetic field: a review. *Int J Heat Mass Transf*. 2017;115:1203-1233. https://doi.org/10.1016/j.ijheatmasstransfer.2017.08.108
22. Gnaneswara Reddy M, Sudharani MVVNL, Ganesh Kumar K, Chamkha AJ, Lorenzini G. Physical aspects of Darcy–Forchheimer flow and dissipative heat transfer of Reiner–Philippoff fluid. *J Therm Anal Calorim*. 2020;141(2):829-838. https://doi.org/10.1007/s10973-019-09072-0
23. Rasool G, Zhang T, Chamkha AJ, Shafiq A, Tlili I, Shahzadi G. Entropy generation and consequences of binary chemical reaction on MHD Darcy–Forchheimer Williamson nanofluid flow over non-linearly stretching surface. *Entropy*. 2019;22(1):e18. https://doi.org/10.3390/e22010018
24. Khan MI, Alzahrani F, Hobiny A, Ali Z. Fully developed second order velocity slip Darcy-Forchheimer flow by a variable thicked surface of disk with entropy generation. *Int Commun Heat Mass Transf*. 2020;117:e104778. https://doi.org/10.1016/j.icheatmasstransfer.2020.104778
25. Hayat T, Khan SA, Alsaedi A, Zia QMZ. Irreversibility analysis in Darcy-Forchheimer flow of CNTs with dissipation and Joule heating effects by a curved stretching sheet. *Appl Nanosci*. 2021;11(1):187-198. https://doi.org/10.1007/s13204-020-01566-w
26. Rao MVS, Gangadhar K, Chamkha AJ, Surekha P. Bioconvection in a convectional nanofluid flow containing gyrotactic microorganisms over an isothermal vertical cone embedded in a porous surface with chemical reactive species. *Arab J Sci Eng*. 2021;46(3):2493-2503. https://doi.org/10.1007/s13369-020-05132-y
27. Raees A, Xu H, Sun Q, Pop I. Mixed convection in gravity-driven nano-liquid film containing both nanoparticles and gyrotactic microorganisms. *Appl Math Mech.-Engl*. Ed. 2015;36(2):163-178. https://doi.org/10.1007/s10483-015-1901-7
28. Narsimulu G, Gopal D, Udaikumar R. Numerical approach for enhanced mass transfer of Bio-convection on Magneto-hydrodynamic Carreau fluid flow through a nonlinear stretching surface. *Mater Today Proc*. 2022;49:2267-2275. https://doi.org/10.1016/j.matpr.2021.09.341
29. Koriko OK, Shah NA, Saleem S, Chung JD, Omowaye AJ, Oreyeni T. Exploration of bioconvection flow of MHD thixotropic nanofluid past a

vertical surface coexisting with both nanoparticles and gyrotactic microorganisms. *Sci Rep*. 2021;11(1):e16627. https://doi.org/10.1038/s41598-021-96185-y

30. Ferdows M, Zaimi K, Rashad AM, Nabwey HA. MHD bioconvection flow and heat transfer of nanofluid through an exponentially stretchable sheet. *Symmetry*. 2020;12(5):e692. https://doi.org/10.3390/sym12050692
31. Balla CS, Ramesh A, Kishan N, Rashad AM, Abdelrahman ZMA. Bioconvection in oxytactic microorganism-saturated porous square enclosure with thermal radiation impact. *J Therm Anal Calorim*. 2020;140(5):2387-2395. https://doi.org/10.1007/s10973-019-09009-7
32. Al-Mubaddel FS, Farooq U, Al-Khaled K, et al. Double stratified analysis for bioconvection radiative flow of Sisko nanofluid with generalized heat/mass fluxes. *Phys Scr*. 2021;96(5):e055004. https://doi.org/10.1088/1402-4896/abeba2
33. Palwasha Z, Islam S, Khan NS, Ayaz H. Non-Newtonian nanoliquids thin-film flow through a porous medium with magnetotactic microorganisms. *Appl Nanosci*. 2018;8(6):1523-1544. https://doi.org/10.1007/s13204-018-0834-5
34. Waqas H, Khan SU, Imran M, Bhatti MM. Thermally developed Falkner-Skan bioconvection flow of a magnetized nanofluid in the presence of a motile gyrotactic microorganism: Buongiorno's nanofluid model. *Phys Scr*. 2019;94(11):e115304. https://doi.org/10.1088/1402-4896/ab2ddc
35. Almeshaal MA, Kalidasan K, Askri F, Velkennedy R, Alsagri AS, Kolsi L. Three-dimensional analysis on natural convection inside a T-shaped cavity with water-based CNT–aluminum oxide hybrid nanofluid. *J Therm Anal Calorim*. 2020;139(3):2089-2098. https://doi.org/10.1007/s10973-019-08533-w
36. Khan SU, Shehzad SA. Analysis for time-dependent flow of Carreau nanofluid over an accelerating surface with gyrotactic microorganisms: model for extrusion systems. *Adv Mech Eng*. 2019;11(12):1-11. https://doi.org/10.1177/1687814019894455
37. Balla CS, Ramesh A, Kishan N, Rashad AM, Abdelrahman ZMA. Bioconvection in oxytactic microorganism-saturated porous square enclosure with thermal radiation impact. *J Therm Anal Calorim*. 2020;140(5):2387-2395. https://doi.org/10.1007/s10973-019-09009-7